

RADIO CONTINUUM OBSERVATIONS TOWARDS OPTICAL AND MOLECULAR OUTFLOWS

José M. Girart,

Departament d'Astronomia i Meteorologia, Universitat de Barcelona

Salvador Curiel,

Instituto de Astronomía, UNAM, México D.F.

Luis F. Rodríguez,

Instituto de Astronomía, UNAM, Morelia

and

Jorge Cantó

Instituto de Astronomía, UNAM, México D.F.

Accepted to the RevMexAA, Vol. 38 no. 2, October 2002

RESUMEN

Presentamos observaciones de continuo en varias frecuencias, realizadas con el VLA, en ocho regiones de formación estelar asociadas con flujos moleculares y ópticos: L1489, HH 68-69, HH 94-95, NGC 2264D, L1681B, L778, MWC 1080 y V645 Cyg. Detectamos tres chorros radio térmicos, L1489, YLW 16A en L1681B y NGC 2264D VLA 7, asociados con flujos moleculares y/o flujos HH. Los chorros térmicos de radio en L1489 y NGC 2264D VLA 7 aparecen colimados en la dirección del flujo a mayor escala. Presentamos la primera detección tentativa de un chorro no térmico de radio, L778 VLA 5, asociado con una protoestrella de baja masa de clase I y con un flujo molecular. En HH 68-69, HH 94-95 y en el flujo molecular en NGC 2264D no hemos podido identificar las fuentes de excitación de estos flujos. La emisión de radio asociada con V645 Cyg es bastante extendida, ~ 0.1 pc y variable. Detectamos tres radio fuentes en la región de MWC 1080 que podrían estar asociadas a fuentes jóvenes.

ABSTRACT

We present multi-frequency VLA continuum observations towards 8 star forming regions with molecular and optical outflows: L1489, HH 68-69, HH 94-95, NGC 2264D, L1681B, L778, MWC 1080 and V645 Cyg. We detect three thermal radio jets, L1489, YLW 16A in L1681B and NGC 2264D VLA 7, associated with molecular and/or HH outflows. The L1489 and NGC 2264D VLA 7 thermal radio jets appear elongated in the direction of the larger scale outflow. We report the first tentative detection of a non-thermal radio jet, L778 VLA 5, associated with a low mass Class I protostar and powering a molecular outflow. For HH 68-69, HH 94-95 and the molecular outflow in NGC 2264D we could not identify a candidate of the exciting source of these outflows. The radio emission associated with V645 Cyg is quite extended, ~ 0.1 pc, and time variable. We detect three radio sources in the MWC 1080 that could be associated with YSOs.

Key Words: ISM: INDIVIDUAL: L1489, HH 68-69, HH 94-95, NGC 2264D, L1681B, L778, V645 Cyg, MWC 1080 — ISM: JETS AND OUTFLOWS — STARS: FORMATION

1. INTRODUCTION

It is well established that in the early stages of star formation there is a large mass loss in young stellar objects (YSOs). The two most spectacular manifestations of this phenomenon are the Herbig-Haro (HH thereafter) outflows and the bipolar molecular outflows. HH outflows are shocks excited by highly collimated, fast winds coming from YSO (e.g., Hartigan et al. 2000), while bipolar molecular outflows are likely ambient gas swept up by those highly collimated winds (e.g., Richer et al. 2000). The energy sources of most molecular and HH outflows are surrounded by large amounts of gas and dust, which contribute significantly to their spectral energy distribution and produce such a large extinction that YSOs are generally invisible at optical wavelengths (e.g., André 1997). Sometimes, they are so deeply embedded that in spite of the recent developments in instrumentation at near-infrared wavelengths, they are not easily detected even at these wavelengths (e.g., Lada & Lada 1991). Therefore, observations in the mid and far infrared (and longward) wavelengths are needed to identify the YSOs driving the molecular and HH outflows. Submillimeter and millimeter observations are probably the most useful techniques to identify YSOs, since they usually exhibit strong dust emission at these wavelengths, and the mm interferometers can achieve high angular resolution (e.g., Wilner & Lay 2000; Rodríguez et al. 1998).

An alternative way to identify this type of sources is through interferometric radio continuum observations at centimeter wavelengths, carried out mainly with the VLA (and more recently with MERLIN and the Australia Telescope). The VLA allows to map large regions (e.g. the primary beam at 6 cm is 9') with a very high sensitivity. In addition, the spectral indices of the sources can be measured from multi-frequency radio continuum observations and, therefore, it allows to elucidate the nature of the radio emission. Combining this type of observations with other criteria, such as the source coinciding with the geometrical center of the outflow and its association with an infrared and/or millimeter counterpart, has proven to be a very useful tool to discriminate among the candidates of the energy source of the outflow (e.g., HH 1-2: Pravdo et al. 1985; L1448: Curiel et al. 1990; L1287: Anglada et al. 1994). Recently, a number of surveys at centimeter wavelengths have been carried out in order to identify the powering sources of molecular outflows (e.g., Anglada et al. 1992, 1998; Beltrán 2001) and of HH objects (e.g., Rodríguez & Reipurth 1994, 1998; Avila, Rodríguez,

& Curiel 2001).

For wavelengths longer than ~ 1 cm, the continuum emission of the energy sources of molecular and HH outflows is often dominated by free-free emission from partially ionized outflows (e.g., Anglada 1996). These cm radio observations allow to determine with great accuracy the position of the exciting source and to determine the morphology and other physical parameters of the ionized gas at small angular scales. Thus, the radio continuum sources associated with YSOs, powering molecular and/or HH outflows, are usually found to have the following characteristics (e.g., Anglada 1996, Rodríguez 1997): (1) Relatively weak flux densities in the cm regime (around 1 mJy or less); (2) Spectral indices that are flat or rise slowly with frequency (typically between -0.1 and 1); (3) No evidence of large time variability; (4) No evidence of polarization; and (5) in some of the best studied cases they exhibit a jet-like morphology, with their orientation, in most cases, along the molecular or HH outflow direction. Because of these properties, these objects are known in the literature as “thermal radio jets”.

In this paper we present matching-beam VLA observations at 2 and 6 cm and sub-arcsecond angular resolution observations towards several star forming regions with associated molecular outflows and/or Herbig-Haro objects. Most of the selected regions were previously observed with the VLA at only one wavelength and with lower angular resolution.

2. OBSERVATIONS

The radio continuum observations were carried out towards 8 fields with the Very Large Array (VLA) of the National Radio Astronomy Observatory¹ between 1989 and 1997. Matching-beam observations at 2 and 6 cm toward HH 94-95, NGC 2264D, L778, V645 Cyg and MWC 1080 were carried out with the D and B/C configurations respectively, which provided an angular resolution of $\sim 5''$. The 2 and 6 cm observations were done with a difference of about half a year. The similar angular resolution and the proximity in time of the observations allow a good estimation of the spectral indices. In addition, sensitive subarcsecond angular resolution observations at 3.6 cm toward L1489, HH 68-69, HH 94-95, NGC 2264D, L1681B and L778 were carried out with the A/B and A configurations. NGC 2264D and V645 Cyg were also observed at 3.6 cm in the D array. The absolute amplitude cali-

¹NRAO is a facility of the National Science Foundation operated under cooperative agreement by Associated Universities, Inc.

TABLE 1
OBSERVED REGIONS

Region	Phase Center		λ cm	Date	Phase Calibrator	Synthesized Beam		rms Noise $\mu\text{Jy beam}^{-1}$
	α (J2000)	δ (J2000)				HPFW	PA	
L1489	04 04 42.9	+26 18 56	3.6	28/05/90	0403+260	$0''.42 \times 0''.29$	-84°	15
HH 68-69	05 41 38.2	-06 27 44	3.6	07/07/95	0550+032	$0''.33 \times 0''.25$	-19°	24
HH 94-95	05 43 39.0	-02 35 09	2	26/01/90	0541-056	$6''.36 \times 4''.87$	-11°	63
			3.6	28/05/90	0541-056	$0''.39 \times 0''.36$	$+72^\circ$	15
			3.6	05/01/97	0539-057	$0''.32 \times 0''.27$	$+25^\circ$	10
			6	31/07/89	0550+032	$6''.88 \times 3''.95$	-30°	34
NGC 2264D	06 41 04.5	+09 36 20	2	26/01/90	0725+144	$5''.74 \times 4''.94$	$+10^\circ$	59
			3.6	16/07/92	0629+104	$10''.15 \times 8''.12$	-9°	42
			3.6	07/07/95	0550+032	$0''.30 \times 0''.25$	-45°	24
			6	31/07/89	0550+032	$4''.74 \times 4''.16$	-34°	41
L1681B	16 27 28.0	-24 39 33	3.6	28/05/90	1626-298	$0''.51 \times 0''.21$	$+23^\circ$	17
L778	19 26 28.9	+23 56 53	2	26/01/90	1923+210	$5''.27 \times 4''.89$	-3°	57
			3.6	28/05/90	1923+210	$0''.36 \times 0''.27$	$+49^\circ$	16
			6	27/07/89	1923+210	$4''.43 \times 3''.91$	-25°	33
V645 Cyg	21 39 58.1	+50 14 20	2	26/01/90	2200+420	$5''.37 \times 4''.95$	$+12^\circ$	66
			3.6	31/01/94	2146+608	$11''.1 \times 10''.6$	-66°	30
			6	27/07/89	2200+420	$4''.72 \times 4''.30$	$+15^\circ$	32
MWC 1080	23 17 27.4	+60 50 48	2	26/01/90	0014+612	$5''.88 \times 4''.90$	-2°	80
			6	27/07/89	2352+495	$5''.50 \times 5''.03$	$+55^\circ$	35

brator was always 3C286. The data were edited and calibrated following the standard VLA procedures with the AIPS software package. In NGC 2264D a strong source was detected at 6 cm, outside the primary beam response (HPFW) (at $\sim 10^\circ\text{E}$ and 11°N from the phase center). This source was removed from the u, v data following the recommended procedure (map done using UVMAP with a shift of $x = -596''$, $y = 648''$, cleaned with APCLN and subtracting the cleaned components from the u, v data using UVSUB). Self-calibration was performed on those fields with strong sources ($\gtrsim 5$ mJy): L778, V645 Cyg and NGC 2264D at 6 cm. Final maps were done using robust weighting of ~ 0.5 for the subarcsecond 3.6 cm observations and using natural weighting for the rest of the observations. All the fluxes were corrected by the VLA antenna primary beam response. In Table 1 we list the observed regions, the phase center, the phase calibrators, the synthesized beam and the rms noise achieved for all the fields. The measured positions and fluxes of the sources detected with the 2 and 6 cm matching-beam observations are given in Table 2. The positions and flux densities of the 3.6 cm subarcsecond and low angular resolution observations are given in Table 3 and 4, respectively. The fluxes and spectral indices of the candidates for driving source, obtained from the matching-beam observations, are shown in Table 5. The deconvolved size, the position angle and the projected physical size of the putative driving

sources that were spatially resolved at 3.6 cm are also shown in Table 5.

Compared with the 2 and 3.6 cm maps, the 6 cm maps are more affected by the presence of background sources due to the larger primary beam ($\sim 9'$) and the increasing flux density with wavelength of these non-thermal sources. In order to identify them we have defined possible background sources as those which lie farther than $2'$ from the phase center (and therefore far away from the geometrical center of the molecular or optical outflow), and those which exhibit a clearly non-thermal emission (i.e., a negative spectral index). In addition, we looked for 20 cm counterparts using the NVSS (NRAO VLA Sky Survey) catalog (Condon et al. 1998) since non-thermal sources are stronger at this wavelength. We note that with these criteria, we do not expect to identify all the non-thermal sources within the 6 cm primary beam, since we cannot determine a spectral index for all the sources due to the significantly lower sensitivity of the 20 cm maps. The sources that meet these criteria are labeled as background, except for those which have a tentative identification at other wavelengths (see Tables 2, 3 and 4). We detected a total of 30 radio continuum sources in the 5 fields observed at 6 cm with a peak flux above the $5\text{-}\sigma$ level, and 21 of them are identified as background sources. The number of background sources expected within the VLA primary beam at 6 cm can be estimated from the formulation given

TABLE 2
SOURCES DETECTED FROM THE MATCHING-BEAM OBSERVATIONS^a

Region	VLA	α (J2000)	δ (J2000)	6 cm Flux (mJy)	2 cm Flux (mJy)	Identification
HH 94-95:	(1)	05 43 28.36	-02 35 26.3	0.50 ± 0.09	<i>opb</i>	<i>bg</i>
	(2)	05 43 39.18	-02 35 10.1	0.30 ± 0.07	0.39 ± 0.12	
	(4)	05 43 57.60	-02 34 54.4	1.53 ± 0.07	<i>opb</i>	
	(5)	05 44 15.50	-02 45 35.1	^b	<i>opb</i>	<i>bg</i>
	(6)	05 44 47.19	-02 35 06.1	^b	<i>opb</i>	PMN J0544-0234?
NGC 2264D:	(1)	06 40 48.14	+09 33 05.0	3.6 ± 0.3	<i>opb</i>	<i>bg</i>
	(2)	06 40 50.47	+09 32 19.6	0.9 ± 0.2	<i>opb</i>	<i>bg</i>
	(3)	06 40 51.96	+09 31 54.0	18.6 ± 0.3	<i>opb</i>	<i>bg</i>
	(4)	06 40 52.64	+09 29 54.0	20.0 ± 0.5	<i>opb</i>	<i>bg</i>
	(5)	06 40 56.91	+09 38 42.1	2.78 ± 0.08	<i>opb</i>	<i>bg</i>
	(7)	06 41 04.52	+09 36 20.5	0.72 ± 0.04	1.12 ± 0.08	
	(12)	06 41 45.14	+09 47 03.0	^b	<i>opb</i>	4C09.25
L778:	(1)	19 26 02.69	+23 55 07.1	10.8 ± 0.1	<i>opb</i>	<i>bg</i>
	(2)	19 26 02.76	+23 54 57.1	11.0 ± 0.1	<i>opb</i>	<i>bg</i>
	(3)	19 26 12.64	+23 54 01.8	1.0 ± 0.1	<i>opb</i>	<i>bg</i>
	(4)	19 26 22.84	+23 53 46.8	0.3 ± 0.1	<i>opb</i>	<i>bg</i>
	(5)	19 26 28.77	+23 56 52.7	1.01 ± 0.05	0.22 ± 0.06	IRAS 19243+2350
	(6)	19 26 29.15	+23 56 18.6	0.71 ± 0.05	0.79 ± 0.09	
	(7)	19 26 30.11	+23 55 14.0	8.83 ± 0.06	2.66 ± 0.24	<i>bg</i>
V645 Cyg:	(1)	21 39 22.60	+50 16 58.7	8.2 ± 0.2	<i>opb</i>	<i>bg</i>
	(2)	21 39 22.86	+50 10 24.7	4.4 ± 0.3	<i>opb</i>	<i>bg</i>
	(3)	21 39 32.92	+50 09 08.5	3.1 ± 0.2	<i>opb</i>	IRAS 21377+4955
	(4)	21 39 33.36	+50 09 10.8	2.1 ± 0.3	<i>opb</i>	<i>id.</i>
	(5)	21 39 43.62	+50 15 16.8	1.72 ± 0.06	<i>opb</i>	<i>bg</i>
	(6)	21 39 58.24	+50 14 21.5	0.57 ± 0.04	1.04 ± 0.22	V645 Cyg
	(7)	21 40 00.32	+50 06 51.6	3.9 ± 0.5	<i>opb</i>	<i>bg</i>
	(8)	21 40 00.87	+50 13 39.6	8.43 ± 0.06	2.89 ± 0.15	<i>bg</i>
MWC 1080:	(1)	23 16 46.83	+60 53 19.9	4.1 ± 0.2	<i>opb</i>	<i>bg</i>
	(2)	23 17 20.36	+60 48 20.8	0.43 ± 0.08	<i>opb</i>	<i>bg</i>
	(3)	23 17 24.14	+60 50 44.9	0.17 ± 0.04	$\lesssim 0.32$	
	(4)	23 17 25.52	+60 50 42.9	0.21 ± 0.07	$\lesssim 0.32$	MWC 1080?
	(5)	23 17 27.43	+60 50 48.9	0.20 ± 0.05	$\lesssim 0.32$	
	(6)	23 17 34.48	+60 56 43.1	~ 18	<i>opb</i>	<i>bg</i>

^a “*opb*” indicates sources outside of the 2 cm primary beam. “*bg*” means a likely background source.

^b Sources outside the primary beam at 6 cm.

by Anglada et al. (1998):

$$\langle N \rangle \simeq 1.1 (S_0/mJy)^{-0.75} \quad (1)$$

For our typical detection threshold (0.18 mJy at 5σ) we expect to detect about 20 sources for the five fields, which is in agreement with our initial estimate of 21 background sources.

Since the thermal radio jets are typically weak sources, in order to elucidate whether they are resolved at subarcsecond angular resolutions, we use $S_{\text{total}} - S_{\text{peak}} \gtrsim 2 \times (\Delta S_{\text{total}} + \Delta S_{\text{peak}})$ as a criteria, where S_{total} and S_{peak} are the total flux density and the peak intensity respectively, and ΔS_{total} and ΔS_{peak} are their respective rms noises. For those sources with adequate signal-to-noise ratio ($SNR \gtrsim 8$) least-square fits of Gaussian ellipsoids were done to obtain the deconvolved size and the position angle

(PA) of the source. We have taken into account the beam smearing that affects the sources which are far from the phase center, producing an apparent elongation in the direction toward the phase center of approximately $[\frac{d}{r}] \times \frac{\Delta\nu}{\nu}$, where d is the distance to the phase center, ν and $\Delta\nu$ are the observed frequency and bandwidth, respectively .

3. RESULTS AND DISCUSSION

3.1. L1489

L1489 is a well studied dark cloud located in the Taurus molecular cloud complex (e. g., Myers et al. 1988; Zhou et al. 1989; Miyawaki & Hayashi 1992). Embedded in the dark cloud there is a Class I YSO with a luminosity of $3.7 L_{\odot}$, surrounded by an optical and near-IR nebulosity (e. g., Myers et al. 1987; Zinnecker et al. 1992; Heyer et al. 1990). High an-

TABLE 3
SOURCES DETECTED AT 3.6 CM (A AND A/B ARRAY)

Object	α (J2000)	δ (J2000)	Flux (mJy)	Identification ^a
L1489:				
1	04 04 43.088	+26 18 56.76	0.49 ± 0.02	IRAS 04016+2610
HH 68-69:				
1	05 41 45.802	-06 27 05.78	1.30 ± 0.05	
HH 94-95:				
1	05 43 28.337	-02 35 25.88	0.60 ± 0.05	<i>bg</i>
2	05 43 39.168	-02 35 09.51	0.29 ± 0.02	
3	05 43 39.295	-02 35 36.39	0.12 ± 0.02	
NGC 2264D:				
5	06 40 56.905	+09 38 42.1	0.9 ± 0.1	<i>bg</i>
7	06 41 04.516	+09 36 20.52	0.62 ± 0.03	
8	06 41 06.503	+09 36 05.28	1.49 ± 0.06	
9	06 41 06.579	+09 34 32.15	0.21 ± 0.06	
10	06 41 06.665	+09 35 30.07	0.20 ± 0.05	
L1681B:				
1	16 27 26.896	-24 40 49.79	1.80 ± 0.03	YLW 15
2	16 27 26.921	-24 40 50.23	0.79 ± 0.03	<i>id.</i>
3	16 27 27.997	-24 39 32.87	0.67 ± 0.03	YLW 16A
L778:				
5	19 26 28.786	+23 56 53.39	0.69 ± 0.02	IRAS 19243+2350
6	19 26 29.143	+23 56 18.76	1.06 ± 0.02	
7	19 26 30.109	+23 55 14.36	5.29 ± 0.03	<i>bg</i>

^a *bg*: likely a background source.

TABLE 4
SOURCES DETECTED AT 3.6 CM (D ARRAY)

Object	α (J2000)	δ (J2000)	Flux (mJy)	Identification ^a
NGC 2264D:				
5	06 40 56.91	+09 38 42.1	2.0 ± 0.2	<i>bg</i>
6	06 41 02.82	+09 36 16.9	0.32 ± 0.04	IRAS 06328+0939
7	06 41 04.52	+09 36 20.5	1.17 ± 0.07	
8	06 41 06.50	+09 36 05.3	~ 0.13	
11	06 41 06.67	+09 35 54.9	0.26 ± 0.04	
V645 Cyg:				
5	21 39 43.54	+50 15 16.7	0.81 ± 0.14	<i>bg</i>
6	21 39 58.21	+50 14 20.9	0.99 ± 0.03	V645 Cyg
8	21 40 00.82	+50 13 39.6	5.57 ± 0.05	<i>bg</i>

^a *bg*: likely a background source.

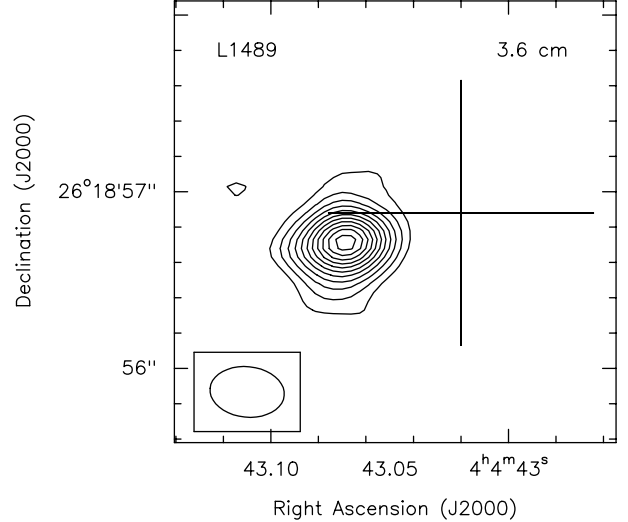


Fig. 1. Subarcsecond angular resolution map at 3.6 cm of L1489. Contours are $-3, 3, 5, 7, 9, \dots$ and 23 times the rms noise of the map, $15 \mu\text{Jy beam}^{-1}$. The half power contour of the synthesized beam is shown in the bottom left corner. The cross marks the position of the molecular disk around the YSO (Hogerheijde et al. 1998).

gular resolution observations show a 2000 AU rotating circumstellar envelope around the YSO (Ohashi et al. 1996; Hogerheijde et al. 1998; Hogerheijde & Sandell 2000). HST observations (Padgett et al. 1999; Wood et al. 2001) revealed a dark dust lane elongated over the east-west direction ($PA = 85^\circ$) with a unipolar nebula with its symmetry axis perpendicular to the dust lane ($PA = 175^\circ$), possibly engulfing an embedded binary system. Associated with this source, there is a low-velocity molecular outflow without a well defined bipolar morphology (Myers et al. 1992), although higher angular resolution observations reveal a weak and compact bipolar component of the molecular outflow coinciding with the YSO and oriented nearly in the north-south direction ($PA = 165^\circ$), i. e., perpendicular to the circumstellar envelope (Hogerheijde et al. 1998). Radio continuum emission arising from the energy source of the L1489 molecular outflow shows that the emission has a positive spectral index, 0.3 ± 0.2 , and is partially resolved in the NW-SE direction at subarcsecond scales (Rodríguez et al. 1989; Lucas et al. 2000). Optical and near-IR emission show a HH system (HH 360 through 362), that also appears to be powered by the same source (Gómez, Whitney & Kenyon 1997; Lucas et al. 2000).

For this source we carried out subarcsecond angular resolution observations at 3.6 cm. The map obtained is shown in Figure 1. The emission is par-

TABLE 5
CANDIDATES OF POWERING MOLECULAR/HH OUTFLOWS

Region	Outflow	Source	VLA Candidate Properties				Comments
			Spectral Index	Deconvolved Size ^a	PA	Size (AU)	
L1489	CO outflow, HH 360	VLA 1	0.3±0.1	0'27(2)×0'15(2)	168°±7°	38	Class I YSO
HH 94-95	HH 94-95	VLA 2	0.0±0.3	∠ 0'1×∠ 0'1	...	∠ 50	Dustless object
		VLA 3	-0.4 to 1.3	∠ 0'3×∠ 0'3	...	∠ 150	Unknown counterpart
		VLA 7	0.4±0.1	0'46(2)×0'27(2)	162°±5°	368	Unknown counterpart
NGC 2264D	HH 125/225/226	VLA 3	0.1±0.1	0'27(2)×0'13(2)	47°±7°	43	Class I YSO
YLW 16A	CO outflow	VLA 5	-0.82±0.04	0'34(1)×0'09(2)	97°±2°	142	Class I YSO?
L778	CO outflow	VLA 6	0.5±0.2	6'5(4)×3'6(4)	7°±6°	23000	Herbig Ae/Be star
V645 Cyg	CO outflow	VLA 4	∠ 0.4	∠ 5''×∠ 5''	...	∠ 13000	Associated with MWC 1080 ?
MWC 1080	HH/CO outflow	VLA 3	∠ 0.6	∠ 5''×∠ 5''	...	∠ 13000	Dusty object
MWC 1080	HH/CO outflow	VLA 5	∠ 0.4	∠ 5''×∠ 5''	...	∠ 13000	Dusty object

^a The value within the parenthesis gives the error in the last digit

tially resolved (see Fig. 1), mainly in the north-south direction, with a peak intensity of 0.35 ± 0.01 mJy beam⁻¹. The deconvolved size from a Gaussian fit is $0''.26 \pm 0''.01 \times 0''.13 \pm 0''.02$ and the position angle of the major axis is $PA = 171^\circ \pm 5^\circ$. The intensity and size measured are in agreement with the values obtained by Lucas et al. (2000). The emission is extended along the outflow axis, defined by the main axis of the compact component of the molecular outflow axis and the line joining the HH 360 knots (Hogerheijde et al. 1998; Gómez et al. 1997), and perpendicular to the molecular and dust circumstellar core that surrounds this YSO (Ohashi et al. 1996; Hogerheijde et al. 1998). We note, however, that HH 361 and HH 362, and the more extended molecular outflow do not line up in the north-south direction (see Fig. 1 from Gómez et al. 1997). This might be due to a change of the outflow direction, or to the presence of a second outflow in the region. Indeed, Lucas et al. (2000) shows that the near-IR H₂ emission traces a quadrupolar outflow.

In order to compare the flux density with previous VLA observations, we made natural weighting maps by applying a Gaussian taper to the visibilities, which provided a $0''.5$ synthesized beam. The total flux density measured from this map is 0.52 ± 0.02 mJy, which is in agreement with the lower angular resolution measurements at 2 and 6 cm by Rodríguez et al. (1989). Combining flux densities obtained at the three wavelengths, we obtain that the spectral index is 0.3 ± 0.1 , which is consistent with partially thick free-free emission.

3.2. HH 68-69

The HH 68-69 objects were discovered by Reipurth & Graham (1988), although this is a poorly studied region. The optical outflow is located in the remains of a molecular cloud, which is probably in the process of destruction due to an expanding HII region (Ogura & Sugitani 1998). Detailed analysis of the IRAS images led Cohen (1990) to suggest that HH 68-69 are two independent HH systems, powered by two infrared sources, IRAS 05391–0627C and IRAS 05393–0632. Rodríguez and Reipurth (1994) and Avila et al. (2001) failed to detect the radio continuum emission towards the infrared sources. Yet, Avila et al. (2001) detected emission towards HH 68b with a flux density of 0.18 mJy.

The subarcsecond angular resolution observations at 3.6 cm failed to detect emission associated with either the infrared sources in this region or with HH 68b, within an upper limit of ~ 0.10 mJy beam⁻¹ (at 4- σ level). Given the quite different angular resolution of Avila et al. (2001) observations, $\sim 3''$, and our observations, the non-detection of HH 68b at subarcsecond angular resolution suggest that the weak emission associated with this HH object is either extended or time variable.

3.3. HH 94-95

HH 94 and 95 are two Herbig-Haro objects (also known as Re 56 and 57), separated by $8'$, located in the L1630 molecular cloud in Orion. The detection of these two HH objects was first reported by Reipurth (1985). HH 95 has a clear bow shock morphology facing away from HH 94, which suggests that both HH objects could be driven by the same source (Reipurth

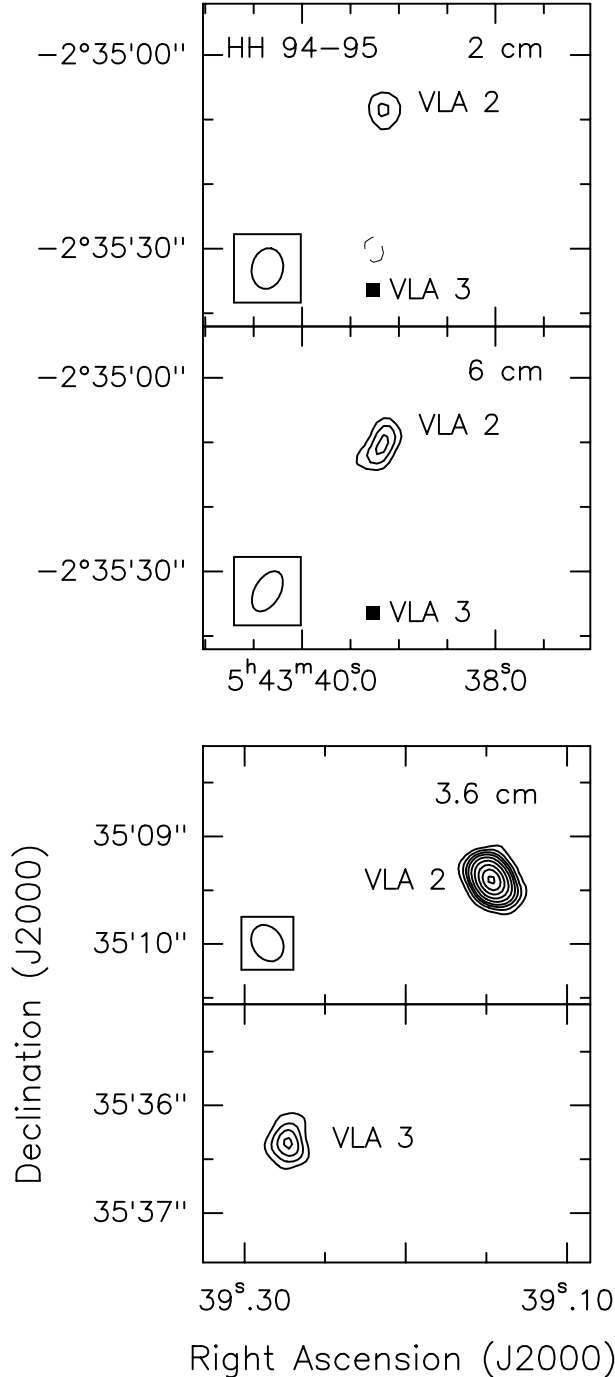


Fig. 2. Composite of VLA maps in the HH 94-95 region: *Two top panels:* 2 cm and 6 cm matching-beam maps. Contours are -3 , -2 , 2 , 3 , 5 , and 7 times the rms of the map, 61 and $36 \mu\text{Jy beam}^{-1}$ at 2 and 6 cm, respectively. *Two bottom panels:* the subarcsecond angular resolution maps at 3.6 cm around VLA sources VLA 2 and VLA 3. Contours are -3 , 3 , 5 , 7 , 9 , 12 , 16 , 21 , 26 , 31 , 36 times the rms of the map, $9 \mu\text{Jy beam}^{-1}$. The half power contour of the synthesized beams are shown in the bottom left corner of each map.

1989). Curiel et al. (1989b) detected a faint radio continuum source located near the geometrical center of this HH system, and proposed it as the powering source of both HH objects. Nevertheless, sensitive mm observations failed to show neither dust emission at this position nor molecular line emission associated with this object (Dent, Matthews & Ward-Thompson 1998).

The matching-beam and the subarcsecond (3.6 cm) radio continuum maps of this region are shown in Figure 2. The 3.6 cm observations were carried out in two epochs, 1990 and 1997. Source VLA 2, the suggested driving source (Curiel et al. 1989b), does not show any variation between these two observations and appears unresolved, with an upper limit of the emitting size of $\sim 0''.1$ or 50 AU. The flux density measured at the three wavelengths observed is consistent with a flat spectrum, $\alpha = 0.0 \pm 0.3$. At about $27''$ south of VLA 2, we have detected a new weak source from our 1997 3.6 cm observations, with a peak intensity of $0.08 \pm 0.01 \text{ mJy beam}^{-1}$ and a total flux density of $0.12 \pm 0.02 \text{ mJy}$. The upper limit for this source from the Curiel et al. (1989b) observations, $\sim 0.09 \text{ mJy beam}^{-1}$ ($5\text{-}\sigma$), is consistent with our observations. Assuming that this source is not variable, the flux measured at 3.6 cm together with the 2 and 6 cm upper limits imply a spectral index between -0.4 and 1.3 .

Given the properties of the emission of sources VLA 2 and VLA 3 and their location close to the geometrical center of the HH 94-95, these two objects are possible powering source candidates. However, Dent et al. (1998) did not detect dust emission towards VLA 2, although their observations did not include VLA 3. A YSO powering an HH system is expected to have detectable dust emission (see Reipurth et al. 1993). Further observations are needed to determine if VLA 3 has dust emission associated, and therefore is the powering source of the HH object.

3.4. NGC 2264D

NGC 2264D is the most massive bipolar molecular outflow located in the Monoceros OB1 molecular cloud (Margulis & Lada 1986). Not far from the geometrical center of this molecular outflow there is an IRAS point source, IRAS 06382+0939, with an infrared luminosity of $\sim 550 L_{\odot}$ (Castelaz & Grasdalen 1988). Far-infrared airborne observations show that the emission extends over several arc minutes (Cohen, Harvey & Schwartz 1985). Mendoza et al. (1990) detected a cluster of near-infrared ob-

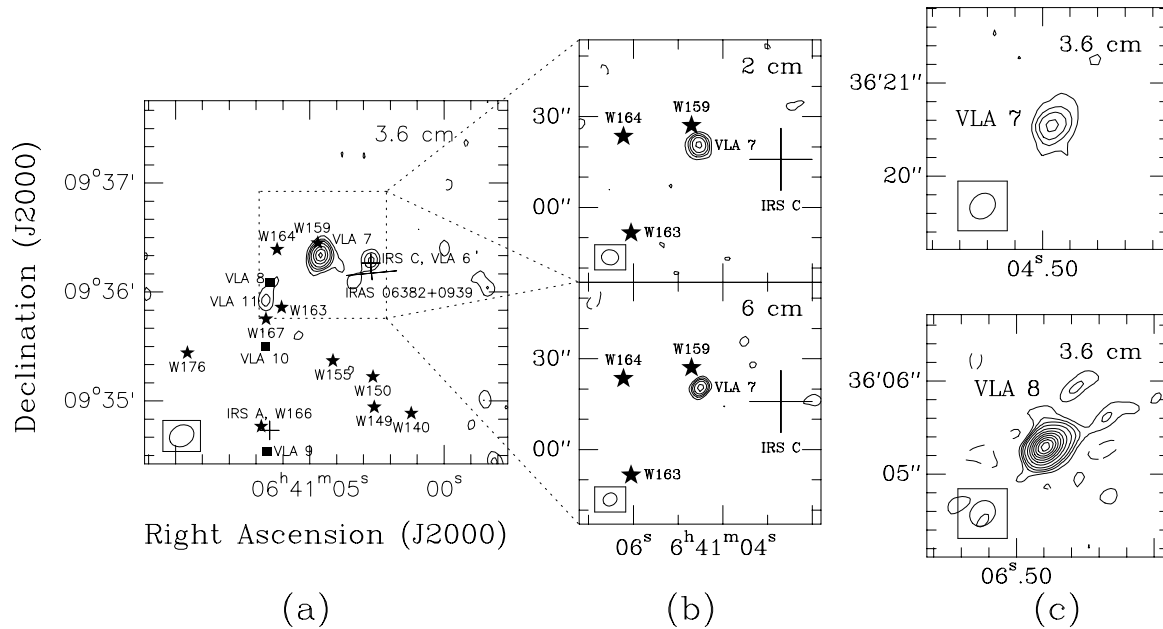


Fig. 3. Composite of VLA maps in the NGC 2264D region: (a) The low angular resolution maps at 3.6 cm, (b) the 2 cm (bottom panel) and 6 cm (top panel) matching-beam maps around VLA 7, (c) Subarcsecond angular resolution map at 3.6 cm around VLA sources VLA 7 (top panel), VLA 8 (bottom panel). Contours are $-3, 3, 5, 7, 10, 15, 20, 25, 30, 35, 40$ and 45 times the rms noise of the maps. The rms of the high and low angular resolution maps at 3.6 cm are 42 and $24 \mu\text{Jy beam}^{-1}$, respectively. The rms for the 2 and 6 cm are $59, 41 \mu\text{Jy beam}^{-1}$, respectively. Position of stars and infrared sources are shown as stars and crosses respectively (López-Molina et al. 1990, Mendoza et al. 1990). The half power contour of the synthesized beams are shown in the bottom left corner of each map.

jects. Four of them are spatially coincident with the molecular outflow. Two of these sources, IRS A and IRS C appear to be close to the geometrical center of the molecular outflow. IRS C is associated with IRAS 06382+0939 and exhibits X-ray emission (Nakano et al. 2000). IRS A is coincident with W166, a Herbig Be/Ae star (Neri, Chavarría-K. & de Lara 1993). Previous VLA observations (Mendoza et al. 1990) showed only one radio continuum source close to the center of the molecular outflow, $\sim 30''$ east from IRAS 06382+0939 (IRS C). To the north of the molecular outflow there are three HH objects (HH 125, HH 225 and HH 226) which are likely part of the same optical outflow system (Walsh, Ogura, & Reipurth 1992). Two infrared objects, IRAS 06382+0939 and IRAS 06382+0945, have been suggested as the driving source of this optical outflow (Cohen, Harvey & Schwartz 1985; Walsh, Ogura, & Reipurth 1992).

From the different observations that we have carried out, we have detected 6 sources towards the center of the molecular outflow (see Table 6 and Figure 3):

Source VLA 6 was detected only in the 3.6 cm low angular resolution map. This source is located $1''.7$ from IRS C. Given the position uncertainties of the

TABLE 6

SOURCES CLOSE TO THE CENTER OF THE MOLECULAR OUTFLOW IN NGC 2264D.

Source	Flux density (mJy) ^a			
	2-cm ($\sim 5''$)	3.6-cm ($\sim 0''.3$)	3.6-cm ($\sim 10''$)	6-cm ($\sim 5''$)
6	$\lesssim 0.25$	$\lesssim 0.09$	0.32 ± 0.04	$\lesssim 0.16$
7	1.12 ± 0.08	0.62 ± 0.08	1.17 ± 0.07	0.72 ± 0.04
8	$\lesssim 0.25$	1.52 ± 0.06	~ 0.13	$\lesssim 0.16$
9	^b	0.21 ± 0.06	$\lesssim 0.24$	$\lesssim 0.18$
10	$\lesssim 0.32$	0.20 ± 0.05	$\lesssim 0.19$	$\lesssim 0.17$
11	$\lesssim 0.26$	$\lesssim 0.10$	0.26 ± 0.04	$\lesssim 0.16$

^a Upper limits are at $4\text{-}\sigma$ level, taking into account the primary beam response.

^b Outside of the HPFW of the primary beam.

infrared position (Castelaz & Grasdalen 1988), these two sources are probably related. The upper limits obtained from the other 3 maps (6, 3.6 and 2 cm) suggest that the emission of this source could be variable, or that the source has a nearly flat spectral index and it is resolved out in the high resolution 3.6 cm observations.

Source VLA 7 is located $\sim 7''$ south of the star W159 (López-Molina, Neri & Chavarría-K. 1990). The position accuracy of the 3.6 cm subarcsecond map ($< 0''.1$) and of the optical image ($< 1''$: López-Molina et al. 1990) suggest that they are probably not associated. No infrared object is associated with this source. The subarcsecond resolution map reveals that source VLA 7 is partially resolved in the north-south direction, with a deconvolved size of $0''.46 \pm 0''.02 \times 0''.27 \pm 0''.02$ and a position angle of $PA = 162^\circ \pm 5^\circ$. From the matching-beam maps we derive a spectral index of $\alpha = 0.4 \pm 0.2$, consistent with it being partially thick thermal emission. The two flux densities measured at 3.6 cm differ by almost a factor 2, which could be the result of the source being partially resolved out in the subarcsecond resolution map or, to variability of this source. Within the uncertainties, the flux density of the lower angular resolution 3.6 cm image is roughly in agreement with the derived matching-beam spectral index.

Sources VLA 8 and VLA 11 were only detected at 3.6 cm (the former in both high and lower angular resolution maps, and the latter only in the lower resolution map). They do not have an optical or infrared counterpart. Source VLA 8 increased its 3.6 cm flux by a factor of 10 between 1992 and 1995. The emission of this source is partially resolved, with a deconvolved size of $0''.21 \pm 0''.01 \times 0''.07 \pm 0''.01$, $PA = 128^\circ \pm 3^\circ$. However, this elongation and orientation is likely due to beam smearing (the source is located $32''$ south-east from the phase center).

Sources VLA 9 and VLA 10 were only marginally detected in the 3.6 cm subarcsecond resolution maps. They do not have any counterpart associated to them, although they appear located within a dense core (Wolf-Chase, Walker, & Lada 1995).

The radio continuum source VLA 7 is a good candidate for the exciting source of the HH 125/225/226 outflow system: it is well aligned with the three HH objects and the emission is partially resolved in the direction of the HH outflow and it has a positive spectral index (derived from the matching-beam observation) which probably indicates free-free emission. Based on its closest location to the geometrical center of the molecular outflow (Mendoza et al.

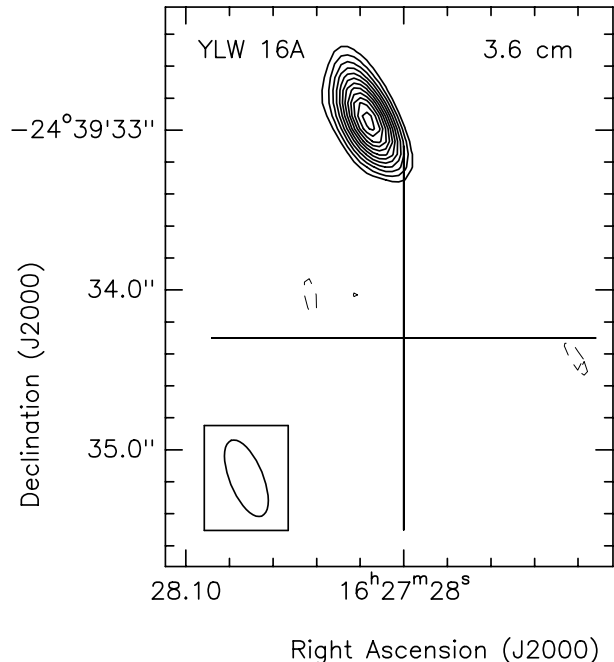


Fig. 4. Subarcsecond angular resolution map at 3.6 cm of YLW 16A. Contours are -3, 3, 5, 7, 9, ... 27 times the rms noise of the map, $17 \mu\text{Jy beam}^{-1}$. The half power contour of the synthesized beam is shown in the bottom left corner. The cross marks the $1\text{-}\sigma$ position uncertainty of the near infrared YSO (Barsony et al. 1997).

1990), IRS A and W166 are also good candidates for powering the molecular outflow. However, we did not detect radio continuum emission associated with these sources. Alternatively, radio sources VLA 9 or VLA 10 could also be candidates for the driving source of the molecular outflow, since they appear to be embedded in a dense core (Wolf-Chase, Walker, & Lada 1995), but further observations are required to confirm the detections.

3.5. L1681B: YLW 16A

YLW 16A (IRS 44) is a Class I source with total luminosity of $13 L_\odot$, located in the L1681B molecular cloud within the ρ Ophiuchi molecular cloud complex (Wilking, Lada & Young 1989; André & Montmerle 1994). It has associated X-ray emission (Casanova et al. 1995; Kamata et al. 1997; Grosso 2001), a compact molecular outflow (Bontemps et al. 1996; Sekimoto et al. 1997) and water masers (Wilking & Claussen 1987). Observations at moderate angular resolution ($\sim 10''$) show there is radio continuum emission associated with YLW 16A (André, Montmerle & Feigelson 1987; Leous et al. 1991).

Figure 4 shows the 3.6 cm subarcsecond resolu-

tion maps of YLW 16A. Within the primary beam we also detected YLW 15, which has been reported by Girart, Rodríguez & Curiel (2000). YLW 16A appears marginally resolved, with a deconvolved size of $0''.27 \pm 0''.02 \times 0''.13 \pm 0''.02$ and a position angle of $47^\circ \pm 7^\circ$. The molecular outflow is close to a pole-on configuration (Sekimoto et al. 1997), so it is difficult to define the axis of symmetry of the molecular outflow in the plane of the sky and compare it with the radio emission elongation direction. In order to compare the VLA flux density of YLW 16A with previous, lower angular resolution measurements, maps were done by applying a Gaussian taper to the visibilities. The flux measured is 0.78 ± 0.06 mJy beam $^{-1}$. This value is consistent with the previous VLA observations (André et al. 1987; Leous et al. 1991; André et al. 1992). From our fluxes and the previous ones obtained at other frequencies we estimate an spectral index of -0.09 ± 0.11 for YLW 16A, which is well consistent with optically thin free-free emission.

3.6. L778

L778 is a dark cloud located in Vulpecula at a distance of about 250 pc (Beichman et al. 1986). It has an ammonia dense core and a complex CO outflow, with two distinct blue lobes and one red lobe (Myers et al. 1988). The infrared source IRAS 19243+2352 is well centered on the core (Myers et al. 1988). Rodríguez et al. (1989) detected three radio continuum sources in this region, one of them within the ellipsoid error of the infrared source IRAS 19243+2352, located $\sim 1''.2$ to the south of IRAS 19243+2352 and the ammonia core. IRAS 19243+2350 appears closer to the geometrical center of the CO molecular outflow, so Rodríguez et al. (1989) suggested that this radio continuum source is also a viable candidate for driving the molecular outflow.

We detected a total of 7 sources in the 6 cm field, including the three radio sources previously reported by Rodríguez et al. (1989). Sources VLA 5 and VLA 6, (see Table 2 and 3) lie close to the center of the molecular outflow. Figure 5 shows the 2 and 6 cm matching-beam and the 3.6 cm subarcsecond resolution maps of these two sources. Source VLA 5, apparently associated with IRAS 19243+2350, is just marginally detected at 2 cm and exhibits a negative spectral index (see Table 5). Its emission is clearly resolved in the 3.6 cm, with an elongated morphology. Its deconvolved size is $\theta_{ds} = 0''.34 \pm 0''.01 \times 0''.09 \pm 0''.02$ (85×23 AU in projection assuming a distance of 250 pc) with a position angle

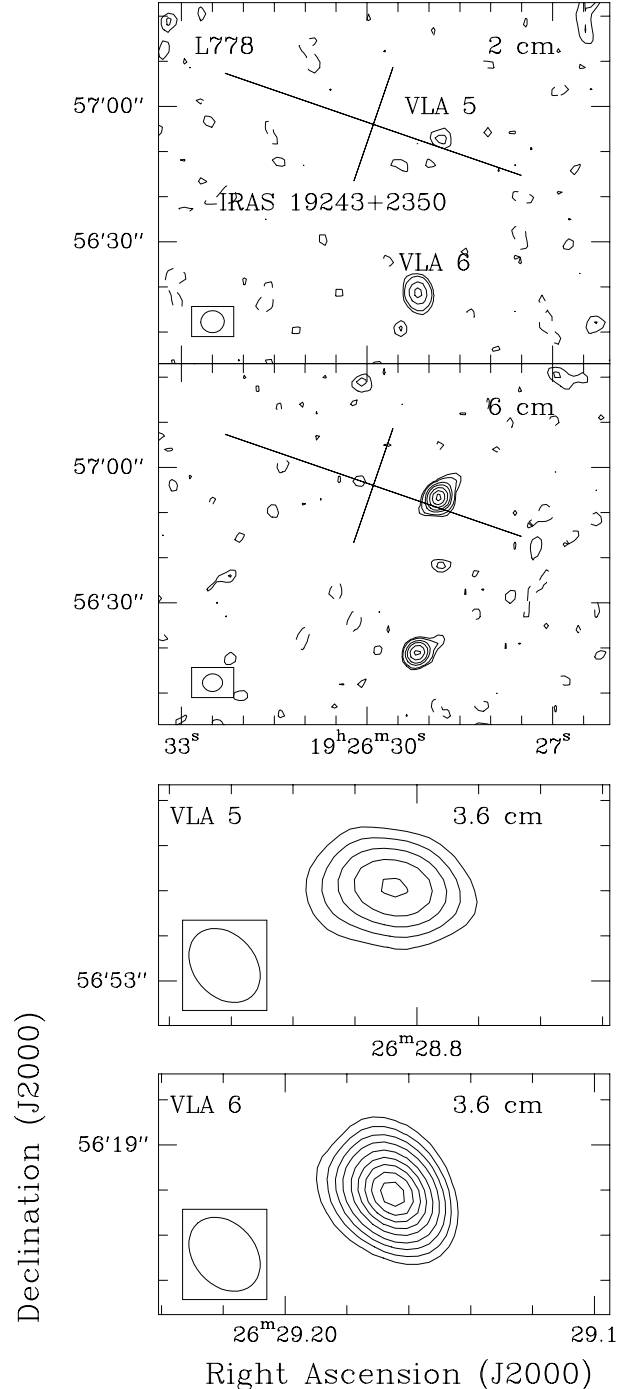


Fig. 5. Composite of VLA maps in the L778 region. *Two top panels:* 2 cm and 6 cm matching-beam maps. Contours are -2, 2, 3, 6, 9, 14, 20 and 26 times the rms of the maps: 57 and 33 μ Jy beam $^{-1}$ at 2 and 6 cm, respectively. *Two bottom panels:* Subarcsecond angular resolution map at 3.6 cm of VLA sources VLA 6 and VLA 5. Contours are 5, 9, 14, 20, 28, 36, 44, 52 and 60 times the rms noise of the maps, 15 μ Jy beam $^{-1}$. The half power contour of the synthesized beams are shown in the bottom left corner of each map.

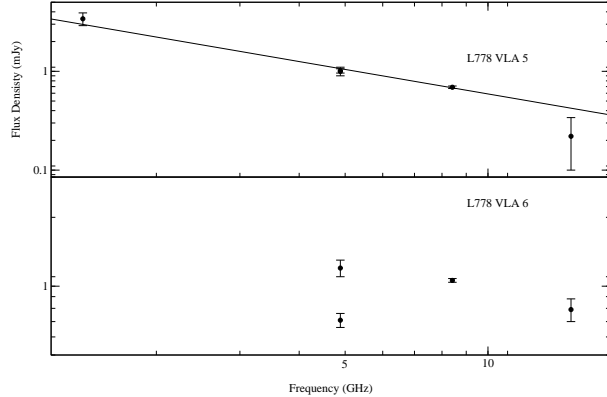


Fig. 6. Centimeter spectrum of VLA 5 (top) and VLA 6 (bottom) in L778. For VLA 6 at 5 GHz the weaker point is from the flux measured in this paper, and the stronger point is the flux measured by Rodríguez et al. (1989). The solid line shows the best fit to the VLA 5 spectral index.

of $PA = 97^\circ \pm 2^\circ$. Source VLA 6 has a positive spectral index (see Table 5) and at high angular resolution appears unresolved. This source has no known counterparts at other wavelengths. Inspection of the 3.6 cm data (the one with the highest sensitivity) around IRAS 19243+2352 and the center of the ammonia core failed to detect any radio continuum source stronger than ~ 0.1 mJy (at $5\text{-}\sigma$ level).

In order to better estimate the spectral indices of the detected sources and check for variability we have taken into account previous measurements by Rodríguez et al. (1989) at 6 cm obtained with a $17''$ angular resolution, and the 20 cm fluxes obtained from the NVSS survey (Condon et al. 1998). The different measurements obtained for source VLA 5 do not suggest variability and are in agreement with a spectral index of $\alpha = -0.82 \pm 0.04$ (see Table 5 and Fig. 6). On the other hand, source VLA 6 is clearly variable (Fig 6), with a 40% change in the flux (at $4\text{-}\sigma$ level) in a period of only 2 years.

Which is the powering source of the molecular L778 outflow? Source VLA 6 is not far from the geometrical center of the southern blue and red lobes (see Myers et al. 1988), however its lack of infrared or submm counterpart and the variability of the radio continuum emission suggest that this source is probably not associated with the molecular outflow. Source 5, associated with IRAS 19243+2350, is elongated roughly in the same direction of the two lobes (blue and redshifted) of the CO molecular outflow. Yet, it has a clearly negative spectral index. One

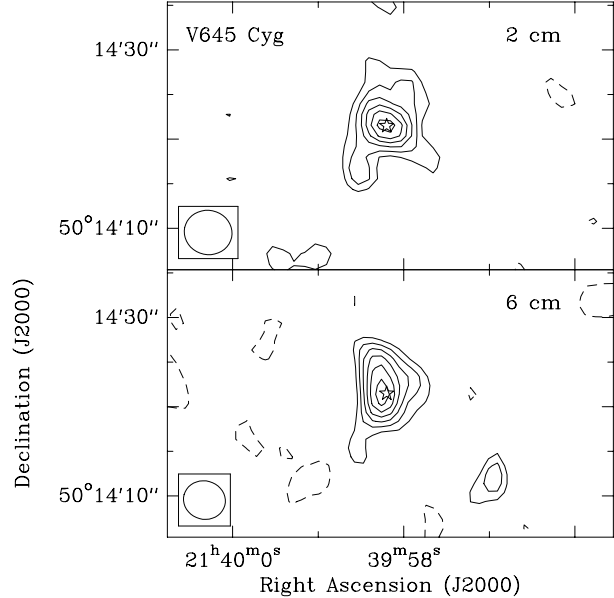


Fig. 7. 2 cm and 6 cm matching-beam maps of V645 Cyg. Contours are -2, 2, 3, 4, 5, 6 and 7 times the rms noise of the maps, which is 66 (2 cm) and $32 \mu\text{Jy beam}^{-1}$ (6 cm). The half power contour of the synthesized beam is shown in the bottom left corner. The stars mark the position of the Herbig Ae/Be star in V645 Cyg.

possibility is that this source is a pre-main-sequence star, since some post T Tauri (Class III) stars exhibit non-thermal emission in the centimeter wavelength (e.g. White et al. 1992). However, the spectral energy distribution of IRAS 19243+2350 (with fluxes of $\lesssim 0.33$, 0.57 , $\gtrsim 0.40$ and 9.10 Jy at 12, 25, 60 and $100 \mu\text{m}$ respectively) are more consistent with a rather younger low mass YSO: a Class I object. Another possibility is that this YSO is powering a synchrotron radio jet, as is the case of the H_2O maser source in W3(OH) (Reid et al. 1995; Wilner, Reid & Menten 1998). This source is a luminous young star that has a synchrotron radio jet with a spectral index of -0.6 ± 0.1 associated to it. This object is well modeled as a biconical synchrotron source tracing a fast well collimated wind (Reid et al. 1995; Wilner, Reid & Menten 1998). However, since there is not known, up to date, a low-mass YSO powering a molecular outflow with this type of emission, further observations are required in order to check whether this mechanism can explain the radio properties of this source or, alternatively, that the radio emission is not associated spatially with the IRAS source.

3.7. V645 Cyg

V645 Cyg is an Herbig Ae/Be object with a spectral type between A0 and A5 and a bolometric luminosity of $4 \times 10^4 [D/3.5\text{Kpc}]^2 L_\odot$, associated with an optical extended nebulosity (e.g., Cohen, 1977; Goodrich 1986; Natta et al. 1993). Two different distances have been used in the bibliography for this object: 6 and 3.5 Kpc. Nevertheless, kinematic and extinction analysis suggest that 3.5 Kpc is the most likely value (Goodrich 1986; Schulz et al. 1989) and this is the value adopted in this paper. The star is surrounded by a high density molecular core of $\sim 80M_\odot$ (e.g., Torrelles et al. 1989; Natta et al. 1993). H_2O and an unusual OH maser emission is associated with this source (Lada et al. 1981; Morris & Kazès 1982). V645 Cyg powers a low velocity bipolar molecular outflow with a modest degree of collimation in the north-south direction (e.g., Verdes-Montenegro et al. 1991). The high luminosity of the source suggests that the radiation field from the star could be driving the molecular outflow (Verdes-Montenegro et al. 1991).

After several unsuccessful attempts (e.g., Kwok 1981; Rodríguez & Cantó 1983), the detection of the radio source associated with V645 Cyg was first reported by Curiel et al. (1989a) from 6 cm VLA observations. They found that the radio source was slightly resolved at an angular resolution of $\sim 10''$. Skinner, Brown & Stewart (1993) confirmed that the radio continuum emission of V645 Cyg is extended, especially in the north-south direction ($\sim 8''.7 \times 6''.6$) and found that the spectral index is almost flat ($\alpha = -0.2 \pm 0.3$).

The matching-beam maps (see Figure 7) show that the emission is partially resolved, especially at 6 cm (see Table 5), and roughly elongated in the North-South direction. A Gaussian fit of the emission at 6 cm gives a deconvolved size of $6''.5 \pm 0''.4 \times 3''.6 \pm 0''.4$ and a position angle of $PA = 7^\circ \pm 6^\circ$. From the matching-beam total fluxes, the derived spectral index is $\alpha = 0.5 \pm 0.2$ (Table 5), which is significantly higher than the one obtained by Skinner et al. (1993).

We carried out additional VLA observations at 3.6 cm in D configuration which provided an angular resolution of $\sim 11''$. The emission is also partially resolved with a deconvolved size of $8''.9 \pm 0''.2 \times 6''.0 \pm 0''.5$ and $PA = 39^\circ \pm 5^\circ$, which is very similar to that obtained by Skinner et al. (1993) and Curiel et al. (1989a) at 6 cm, but slightly larger than the value obtained from the matching-beam 6 cm map. The 3.6 cm flux density, 0.99 ± 0.04 mJy, is inconsistent with the matching-beam flux densities. In Table 7

TABLE 7

OBSERVATIONS OF V645 CYG AT DIFFERENT EPOCHS

Epoch	Angular	Flux density (mJy)		Ref.
	Resolution	3.6-cm	6-cm	
Mar-1980	$0''.5$	-	$\lesssim 0.5$	(1)
Oct-1981	$5''$	-	$\lesssim 1.0$	(2)
Oct-1984	$15''$	-	1.02 ± 0.04	(3) ^a
Jul-1989	$5''$	-	0.57 ± 0.04	(4)
Feb-1990	$0''.3$	$\lesssim 0.11$	-	(5)
Feb-1991	$7''$	0.76 ± 0.15	-	(5)
Feb-1991	$14''$	-	0.87 ± 0.21	(5)
Jun-1991	$14''$	0.70 ± 0.21	-	(5)
Jan-1994	$11''$	0.99 ± 0.04	-	(4)
Jan-1996	$1''.4$	0.55 ± 0.18	-	(6)

References: (1) Kwok 1981, (2) Rodríguez & Cantó 1983, (3) Curiel et al. 1989a, (4) this paper, (5) Skinner et al. 1993, (6) Di Francesco et al. 1997.

^a We re-made the map using natural weighting.

we list the different fluxes measured with the VLA at 3.6 cm and 6 cm, the observing date and the angular resolution of the observations. The data on this table seems to suggest that the flux density decreases with increasing angular resolutions, especially for angular resolution of $\lesssim 5''$. In order to check if the angular resolution is really affecting the matching-beam flux, we assume that the radio emission of V645 Cyg is a Gaussian with a full width at half maximum of the peak emission of $\sim 9''$ (the major axis of the lower angular resolution measurements). The half-power radius in the visibility domain is:

$$r_{(u,v)} = 91.02 \left(\frac{\theta_{\text{FWHM}}}{''} \right)^{-1} \text{ k}\lambda \quad (2)$$

and the fraction of the total flux density observed for a visibility coverage with an inner radius, r_{min} , is:

$$\frac{S_{\text{observed}}}{S_{\text{total}}} = e^{-8.4 \times 10^{-5} (r_{\text{min}}/\text{k}\lambda)^2 (\theta_{\text{FWHM}}/'')^2} \quad (3)$$

The matching-beam observations have a (u, v) coverage radius from ~ 1 to 59 k λ at 6 cm, but it is for a radius $\gtrsim 2$ k λ that the visibility distribution becomes roughly homogeneous in the (u, v) plane. Therefore, using $r_{\text{min}} = 2$ k λ , the flux detected should be 97% of the total flux density at 6 cm. Even for a source of $18''$ we would have detected 90% of the total flux. In addition, we made 6 cm matching-beam maps by applying a Gaussian taper of 25 k λ in the (u, v) plane, which provided a synthesized beam of $\sim 8''$. The new estimated flux densities do not show any significant change at $1-\sigma$ level (0.04 mJy beam $^{-1}$). Therefore, we conclude that the

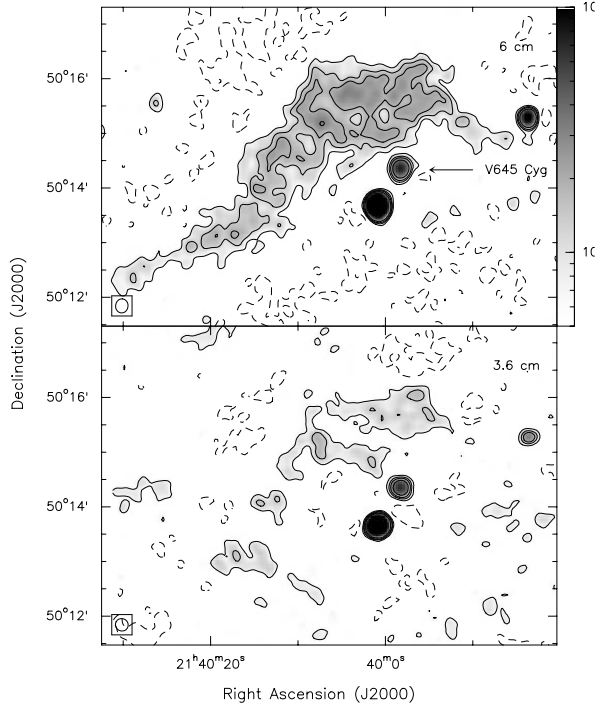


Fig. 8. Cleaned, natural-weight D configuration VLA maps of the V645 Cyg region at 3.6 cm (bottom panel) and 6 cm (top panel). Contours are -4, -2, 2, 4, 6, 10, 15 and 20 times the rms noise of the maps, 34 and $32 \mu\text{Jy beam}^{-1}$ respectively. The half power contour of the synthesized beam is shown in the bottom left corner.

fluxes measured from the matching-beam observations are not underestimated. Thus, the differences observed in the flux density measured at 6 cm (see Table 7), especially between the Oct-1984 and Jul-1989 observations (about $0.45 \pm 0.06 \text{ mJy}$), are likely to be due to time variability. We speculate that the variations in flux density and size observed in this source could be the result of episodic ejection of material by the powering source. Another possibility is that the ionized gas associated with this source can recombine in timescales of a few years, which implies electron densities in excess of $3 \times 10^4 \text{ cm}^{-3}$. Further observations will be needed to test these possibility.

Other objects in the field:

From the VLA D configuration 6 cm map, we detect an extended source close to V645Cyg with a size of $\sim 6' \times 2'$ (see Figure 8) and a total flux density of $31 \pm 1 \text{ mJy}$. The position of this source coincides with the radio object BWE 2138+5001 detected at 6 cm by Becker, White & Edwards (1991) from low angular resolution ($\sim 3'/5$), single dish observations. Using data from the NVSS (NRAO VLA

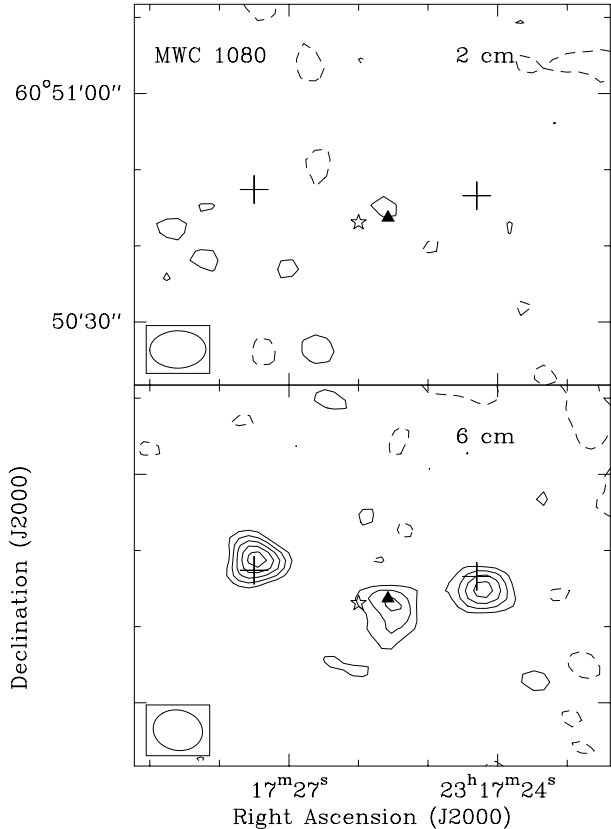


Fig. 9. 2 cm (top panel) and 6 cm (bottom panel) matching-beam maps of MWC 1080. Contours are -2, 2, 3, 4, 5, 6 and 7 times the rms noise of the maps, 80 and $35 \mu\text{Jy beam}^{-1}$ at 2 and 6 cm, respectively. The half power contour of the synthesized beam is shown in the bottom left corner. The filled triangle marks the position of the 3.6 cm radio source detected by Skinner, Brown & Linsky (1990). The star marks the position of the Herbig Ae/Be star in MWC 1080 (Hillenbrand et al. 1992). The two crosses mark the position of dust emission peaks (Fuente et al. 1998).

Sky Survey) survey (Condon, et al. 1998), we obtain that BWE 2138+5001 has a flux density of 34 ± 3 at 20 cm. The estimated spectral index between 6 and 20 cm ($\alpha = -0.1 \pm 0.1$) for this extended object appears to be consistent with this source being an optically thin HII region.

3.8. MWC 1080

MWC 1080 is another Herbig Ae/Be star with an A1 spectral type and a bolometric luminosity of $\sim 8 \times 10^3 L_{\odot}$ associated with an optical nebulosity (e.g., Yoshida et al. 1992; Hillenbrand et al. 1992 and references therein) and located at a distance of about 2.5 Kpc. MWC 1080 is, in fact, a triple sys-

tem (Pirzkal, Spillar & Dyck 1997; Leinert, Richichi & Haas 1997) that has faint X-ray emission (Zinnecker & Preibisch 1994). MWC 1080 shows several signposts of strong mass loss: strong P Cygni profiles in the Balmer lines (e. g., Herbig 1960; Yoshida et al. 1992), a powerful molecular outflow (e. g., Cantó et al. 1984; Levreault 1988), a poorly collimated but extremely fast ($v_{H\alpha}$ up to 1100 km s^{-1}) HH bipolar outflow (e. g., Poetzel, Mundt & Ray 1992). The molecular cloud associated with MWC 1080 has several hundreds of solar masses (e. g., Yoshida et al. 1991), while, from dust emission observations, the circumstellar material around MWC 1080 has only a few solar masses (Mannings 1994; Fuente et al. 1998).

Curiel et al. (1989a) detected, from $10''$ resolution observations at 6 cm, a radio source displaced about $13''$ from the star, surrounded by weak extended emission that roughly engulfs the star as well as its associated optical nebulosity. Higher angular resolution observations ($\sim 1''$) by Skinner, Brown & Linsky (1990) detected at 3.6 cm a weak source located at about $2''$ from the optical source.

At 6 cm we detect 3 sources close to MWC 1080 (see Figure 9). These sources coincide in position with the three relative maxima of the extended radio emission detected at lower angular resolution by Curiel et al. (1989a, see Fig.2 of their paper). Curiel et al. (1989a) estimated a total flux of $\sim 2 \text{ mJy}$ for the extended radio emission, which is significantly higher than the $0.53 \pm 0.08 \text{ mJy}$ flux density measured in our 6 cm maps. This is probably because we are resolving out the weak extended component detected by Curiel et al. (1989a). VLA 4 coincides with the position given by Skinner et al. (1990), but it is located about $3''.5$ west of MWC 1080, so its direct association with the Herbig Ae/Be star is unclear. However, the presence of a strong HH outflow in the east-west direction associated with MWC 1080 (Poetzel, Mundt & Ray 1992) suggests that the emission could be related with the optical outflow. None of the three 6 cm source were detected at 2 cm up to a $3 - \sigma$ level of $0.24 \text{ mJy beam}^{-1}$. This implies that they have a spectral index smaller than 0.6. Interestingly, two relative intensity peaks of the dust continuum emission, at 1.3 mm, mapped by Fuente et al. (1998) seem to coincide in position with the two strongest radio components associated with MWC 1080 (Fig. 9). This suggests that these two radio continuum sources may trace embedded, very young stellar objects.

4. SUMMARY AND CONCLUSIONS

Table 5 shows the radio continuum candidates to power the molecular and/or HH outflows in the regions observed with the VLA. Of the observed regions, HH 68-69 is the only one that is not shown in this table because of the lack of radio continuum emission from our observations. The main results from our observations are:

(1) We detected three radio sources, whose properties are consistent with being thermal radio jets: L1489, NGC 2264D VLA 7 and YLW 16A. The length of these radio jets are $\sim 40 \text{ AU}$ for L1489 and YLW 16A and $\sim 370 \text{ AU}$ for NGC 2264D VLA 7, which are typical values for this type of objects (Anglada 1996). These three radio jets are associated with HH and molecular outflows. L1489 coincides with a compact molecular outflow (Hogerheijde et al. 1998) and with HH 360 (Gómez et al. 1997). NGC 2264D VLA 7 is associated with the system HH 125/225/226 (Walsh, Ogura, & Reipurth 1992). For these two regions, the thermal radio jet is well aligned with the molecular or HH outflow. The thermal radio jet in YLW 16A is associated with a pole-on molecular outflow (Sekimoto et al. 1997).

(2) We detected a non-thermal radio jet in L778 that appears to be associated with a Class I infrared source, IRAS 19243+2350. This radio jet is elongated in the direction of a pair of red and blue high velocity CO lobes (Myers et al. 1988) centered roughly in IRAS 19243+2350. Thus, we suggest the first tentative detection of a non-thermal radio jet associated with a low mass protostar.

(3) Our observations could not find clear candidates for the HH 94-95 system and the molecular outflow in NGC 2264D. In both regions there are several radio sources that could trace the powering source of the outflows, but the lack of known counterpart or the incomplete information of their radio emission properties does not allow to discriminate between them.

(4) V645 Cyg shows radio emission with striking properties: its emission is quite extended, $\sim 23000 \text{ AU}$, but at the same time it is variable. There is also an extended source that appears to be an optically thin HII region.

(5) There is a $\sim 3''.5$ offset between the optical source MWC 1080 and VLA 4, so it is not clear if VLA 4 is directly associated with the star. There are two other radio sources, VLA 3 and 5, that are associated with mm sources and could be tracing protostars.

JMG acknowledges support by RED-2000 from

the Generalitat de Catalunya and by DGICYT grant PB98-0670 (Spain). JMG thanks the hospitality and support of the Instituto de Astronomía-UNAM. SC and LFR acknowledge support from DGAPA, UNAM and CONACyT, México. JC acknowledges support from CONACyT grants 34566-E and 36573-E.

REFERENCES

- André, P. & Montmerle, T. 1994, ApJ, 420, 837
 André, P., Montmerle, T., & Feigelson, E. D. 1987, AJ, 93, 1182
 André, P. 1997, in *Herbig-Haro Flows and the Birth of the Low Mass Stars*, IAU Symposium n.182, B. Reipurth, & C. Bertout (eds.), p. 483
 Anglada, G. 1996, in *Radio Emission from Stars and the Sun*, ASP Conf. Ser. Vol. 93, A. R. Taylor & J. M. Paredes, 3
 Anglada, G., Rodríguez, L. F., Cantó, J., Estalella, R., & Torrelles, J. M. 1992, ApJ, 395, 494
 Anglada, G., Rodríguez, L. F., Girart, J. M., Estalella, R., & Torrelles, J. M. 1994, ApJ, 420, L91
 Anglada, G., Villuendas, E., Estalella, R., Beltrán, M. T., Rodríguez, L. F., Torrelles, J. M., & Curiel, S. 1998, AJ, 116, 2953
 Avila, R., Rodríguez, L. F., & Curiel, S. 2001, RevMexAA, 37, 201
 Barsony, M., Kenyon, S. J., Lada, E. A., & Teuben, P. J. 1997, ApJS, 112, 109
 Beichman, C. A., Myers, P. C., Emerson, J. P., Harris, S., Mathieu, R., Benson, P. J., & Jennings, R. E. 1986, ApJ, 307, 337
 Becker, R. H., White, R. L., & Edwards, A. L. 1991, ApJSS, 75, 1
 Beltrán, M. T., Estalella, R., Anglada, G., Rodríguez, L. F., & Torrelles, J. 2001, AJ, 121, 1556
 Bontemps, S., André, P., Tereby, S., & Cabrit, S. 1996, A&A, 858, 872
 Cabrit, S., & André, P. 1991, ApJ, 379, L25
 Casanova, S., Montmerle, T., Feigelson, E. D., André, P. 1995, ApJ, 439, 752
 Cantó, J., Rodríguez, L. F., Calvet, N., & Levreault, R. M. 1984, ApJ, 282, 631
 Castelaz, M. W., & Grasdalen, G. 1988, ApJ, 335, 150
 Condon, J. J. 1984, ApJ, 287, 461
 Condon, J. J., Cotton, W. D., Greisen, E. W., Yin, Q. F., Perley, R. A., Taylor, G. B., & Broderick, J. J. 1998, AJ, 115, 1693
 Cohen, M., 1977, ApJ, 215, 533
 Cohen, M. 1990, ApJ, 354, 701
 Cohen, M., Harvey, P. M., & Schwartz, R. D. 1985, ApJ, 296, 633
 Curiel, S., Raymond, J. C., Rodríguez, L. F., Cantó, J., & Moran, J. M. 1990, ApJ, 365, L85
 Curiel, S., Rodríguez, L. F., Cantó, J., Bohigas, J., Roth, M., & Torrelles, J. M. 1989a, Ap. Lett. Comm., 27, 299
 Curiel, S., Rodríguez, L. F., Cantó, J., & Torrelles, J. M. 1989b, RevMexAA, 17, 137
 Davis, C. J., & Eislöffel, J. 1995, ApJ, 443, L41
 Dent, W. R. F., Matthews, H. E., & Ward-Thompson, D. 1998, MNRAS, 301, 1049
 Di Francesco, J., Evans II, N. J., Harvey, P. M., Mundy, L. G., Guilloteau, S., & Chandler, C. 1997, ApJ, 482, 433
 Fuente, A., Martín-Pintado, J., Bachiller, R., Neri, R., & Palla, F. 1998, A&A, 334, 253
 Girart, J. M., Rodríguez, L. F., & Curiel, S. 2000, ApJ, 544, L153
 Gómez, J. F., Curiel, S., Torrelles, J. M., Rodríguez, L. F., Anglada, G., & Girart, J. M. 1994, ApJ, 438, 749
 Gómez, M., Whitney, B. A., Kenyon, S. J. 1997, AJ, 114, 1138
 Goodrich, R. W. 1986, ApJ, 311, 882
 Grosso, N. 2001, A&A, 370, L22
 Hartigan, P., Bally, J., Reipurth, B. & Morse, J. 2000, in *Protostars and Planets IV*, V. Mannings, A. Boss & S. Russell (eds.), (University of Arizona Press), p. 841
 Herbig, G. H. 1960, ApJSS, 337
 Heyer, M. H., Ladd, E. F., Myers, P. C., & Campbell, B. 1990, AJ, 99, 1585
 Hillenbrand, L. A., Strom, S. E., Vrba, F. J., & Keene, J. 1992, ApJ, 397, 613
 Hogerheijde, M. R., van Dishoeck, E. F., Blake, G. A., & van Langevelde, H. J. 1998, ApJ, 502, 315
 Hogerheijde, M. R., & Sandell, G. 2000, ApJ, 534, 880
 Kamata, Y., Koyama, K., Tsuboi, Y., Yamauchi, S. 1997, PASJ, 49, 461
 Kwok, S. 1981, PASP, 93, 361
 Lada, C. J., & Lada, E. A. 1991, in *The formation and evolution of stars clusters*, p.3
 Lada, C. J., Blitz, L., Reid, M. J., Moran, J. M. 1981, ApJ, 243, 769
 Leinert, C., Richichi, A., & Haas, M. 1997, A&A, 318, 472
 Leous, J. A., Feigelson, E. D., André, P., & Montmerle, T. 1991, ApJ, 379, 683
 Levreault, R. M. 1988, APJSS, 67, 283
 López-Molina, M. G., Neri, L., & Chavarría-K., C. 1990, RevMexAA, 20, 113
 Lucas, P. W., Blundell, K. M., & Roche, P. F. 2000, MNRAS, 318, 526
 Mannings, V. 1994, MNRAS, 271, 587
 Margulis, M., & Lada, C. J. 1986, ApJ, 309, L87
 Margulis, M., Lada, C. J., & Snell, R. L. 1988, ApJ, 333, 316
 Mendoza, E. E., Rodríguez, L. F., Chavarria, C., & Neri, L. 1990, MNRAS, 246, 518
 Miyawaki, R., & Hayashi, M. 1992, PASJ, 44, 557
 Morris, M., & Kazès, I. 1981, A&A, 111, 239
 Myers, P. C., Fuller, G. A., Mathieu, R. D., Beichman, C. A., Benson, P. J., Schild, R. E., & Emerson, J. P. 1987, ApJ, 319,340
 Myers, P. C., Heyer, M., Snell, R. L., & Goldsmith, P.

- F. 1988, ApJ, 324, 907
- Nakano, M., Yamauchi, S., Sugitani, K., & Ogura, K. 2000, PASJ, 52, 437
- Natta, A., Palla, F., Butner, H.M., Evans II, N. J., & Harvey, P. M. 1993, ApJ, 406, 674
- Neri, L. J., Chavarría-K., C., & de Lara, E. 1993, A&ASS, 102, 201
- Ogura, K., & Sugitani, K. 1998, PASA, 15, 91
- Ohashi, N., Hayashi, M., Kawabe, R., & Ishiguro, M. 1996, ApJ, 466, 317
- Padgett, D. L., Brandner, W., Stapelfeldt, K. R., Strom, S. E., Tereby, S., Koerner, D. 1999, AJ, 117, 1490
- Pirzkal, N., Spillar, E. J., & Dyck, H. M. 1997, ApJ, 481, 392
- Poetzel, R., Mundt, R., & Ray, T. P. 1992, A&A, 262, 229
- Pravdo, S. H., Rodríguez, L. F., Curiel, S., Cantó, J., Torrelles, J. M., Becker, R. H., & Sellgren, K. 1985, ApJ, 293, L35
- Reid, M. J., Argon, A. L., Masson, C. R., Menten, K. M., & Moran, J. M. 1995, ApJ, 443, 238
- Reipurth, B. 1985, A&AS, 61, 319
- Reipurth, B. 1989, A&A, 220, 249
- Reipurth, B., & Graham, J. A. 1988, A&A, 202, 219
- Richer, J., Shepherd, D., Cabrit, S., Bachiller, R., & Churchwell, E. 2000, in *Protostars and Planets IV*, V. Mannings, A. Boss & S. Russell (eds.), (University of Arizona Press), p. 867
- Rodríguez, L. F. 1997, in *Herbig-Haro Flows and the Birth of the Low Mass Stars*, IAU Symposium n.182, B. Reipurth, & C. Bertout (eds.), p. 83
- Rodríguez, L. F., & Cantó, J. 1983, RevMexAA, 8, 163
- Rodríguez, L. F., Myers, P. C., Cruz-González, I., & Tereby, S. 1989, ApJ, 347, 461
- Rodríguez, L. F., & Reipurth, B. 1994, A&A, 281, 882
- Rodríguez, L. F., & Reipurth, B. 1998, RevMexAA, 34, 13
- Rodríguez, L. F. et al. 1998, Nature, 395, 355
- Sekimoto, Y., Tatematsu, K., Umemoto, T., Koyama, K., Tsuboi, Y., Hirano, N., Yamamoto, S. 1997, ApJ, 489, L63
- Skinner, S. L., Brown, A., & Linsky, J. L. 1990, ApJ, 357, L39
- Skinner, S. L., Brown, A., & Stewart, R. T. 1993, ApJSS, 87, 217
- Schulz, A., Black, J. H., Lada, C. J., Ulich, B. L., Martin, R. N., Snell, R. L., & Erickson, N. J. 1989, ApJ, 341, 288
- Stine, P. C., Feigelson, E. D., André, P., & Montmerle, T. 1988, AJ, 96, 1394
- Torrelles, J. M., Verdes-Montenegro, L., Ho, P. T. P., Rodríguez, L. F., & Canto, J. 1989, ApJ, 346, 756.
- Verdes-Montenegro, L., Gómez, J. F., Torrelles, J. M., Anglada, G., Estalella, R., & López, R. 1991, A&A, 244, 84
- Walker, C. K., Adams, F. C., & Lada, C. J. 1990, ApJ, 349, 515
- Walsh, J. R., Ogura, K., & Reipurth, B. 1992, MNRAS, 257, 110
- White, S. M., Pallavicini, R., Kundu, M. R. 1992, A&A, 257, 557
- Wilking, B. A., Lada, C. J., & Young, E. T. 1989, ApJ, 340, 823
- Wilking, B. A., & Claussen, M. J. 1987, 320, L133
- Wilner, D. J., & Lay, O. P. 2000, in *Protostars and Planets IV*, V. Mannings, A. Boss & S. Russell (eds.), (University of Arizona Press), p. 509
- Wilner, D. J., Reid, M. J., Menten, K. M. 1999, ApJ, 513, 775
- Wolf-Chase, G. A., Walker, C. K., & Lada, C. J. 1995, ApJ, 442, 197
- Wood, K., Smith, D., Whitney, B., Stassun, K., Kenyon, S. J., Wolff, M. J., & Bjorkman, K.S. 2001, ApJ, 561, 299
- Yoshida, S. Kogure, T., Nakano, M., Tatematsu, K., & Wiramihardja, S. D. 1991, PASJ, 43, 362
- Yoshida, S. Kogure, T., Nakano, M., Tatematsu, K., & Wiramihardja, S. D. 1992, PASJ, 44, 77
- Zhou, S., Wu, Y., Evans II, N. J., Fuller, G. A., & Myers, P. C. ApJ, 346, 168
- Zinnecker, H., Bastien, P., Arcoragi, J. P. & Yorke, H. W. 1992, A&A, 265, 726
- Zinnecker, H. & Preibisch, T. 1994, A&A, 292, 152

José M. Girart: Departament d'Astronomia i Meteorologia, Universitat de Barcelona, Av. Diagonal 647, 08028 Barcelona, Catalunya, Spain; jgirart@am.ub.es.

Luis F. Rodríguez: Instituto de Astronomía, Universidad Nacional Autónoma de México, A. P. 3-72, (Xangari), 58089 Morelia, Michoacán, México (l.rodriguez@astrosmo.unam.mx)

Salvador Curiel and Jorge Cantó: Instituto de Astronomía, Universidad Nacional Autónoma de México Apdo. Postal 70-264, 04510 México D.F., México, (scuriel@astroscu.unam.mx)